Journal of Guidance, Control, and Dynamics
Vol. 18, No. 5, September–October 1995

Nutational Stability and Passive Control of Spinning Rockets with Internal Mass Motion

D. M. Halsmer
Oral Roberts University, Tulsa, Oklahoma 74171
and
D. L. Mingori
University of California, Los Angeles, Los Angeles, California 90024

Necessary and sufficient conditions for asymptotic stability are developed for a symmetric spinning rocket with axial forcing and dissipative internal mass motion. Results show that spin about the axis of least inertia is asymptotically stable provided that three conditions are satisfied: 1) the axial thrust magnitude is sufficiently large, 2) the restoring forces for the internal mass motion are sufficiently large, and 3) the internal mass motion occurs aft of the system mass center. Under these same conditions, spin about the axis of largest inertia may be unstable. Numerical studies show that a passive control device with these characteristics can be used to attenuate the coning of prolate spinners such as those transfer orbit boost vehicles that have been plagued by unexpectedly pronounced coning instabilities.

Nomenclature

c = damping constant for particle motion
F = magnitude of thrust (assumed constant)
I_1, I_1, I_3 = moments of inertia of (symmetric) rigid body for axes B_1, B_2, and B_3, respectively
k = spring constant for elastic restraint on particle
M = mass of rigid body
m = mass of particle
μ = $m/(m+M)$
Ω = nominal spin rate of rigid body about B_3
ω_1, ω_2 = components of rigid-body angular velocity for axes B_1 and B_2, respectively

Introduction

THIS paper develops analytical stability results and presents a novel approach to passive coning control for symmetric spinning bodies with axial thrust and dissipative internal mass motion. These findings were made while investigating a proposed instability mechanism for the coning anomalies experienced recently on certain transfer orbit boost vehicles such as the PAM-D (Perigee Assist Module-D). It had previously been shown that under certain conditions the coupled effects of internal mass motion and axial thrust are capable of producing coning instabilities similar in character to the observed anomalies.[1] In Ref. 1, the moving mass represented undesirable fluid motion. The present paper does not attempt to further describe the instability mechanism of these anomalies. Instead, it addresses the general behavior of thrusting, spinning bodies with dissipative internal mass motion. Consideration of earlier results presented in Ref. 1 led to the idea that, for a correct choice of parameters, perhaps an internal moving mass could be designed to stabilize an otherwise unstable spinning, thrusting spacecraft. When looked at in this way, it is more appropriate to think of the internal mass as a passive control device similar to the type used to damp nutation in spin-stabilized, nonthrusting spacecraft[2] rather than as a mechanism for instability.

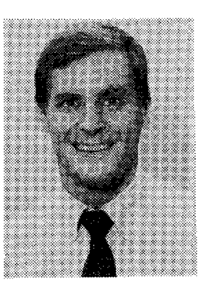

Dominic M. Halsmer was born in Lafayette, Indiana, in 1962. He received the B.S. and M.S. degrees in Aeronautical and Astronautical Engineering from Purdue University, West Lafayette, Indiana, in 1985 and 1986, respectively. He received the Ph.D. degree in Mechanical Engineering from the University of California at Los Angeles in 1992. From 1985 to 1992, he worked as a control systems engineer for Hughes Aircraft Company, Space and Communications Group, in El Segundo, California. He joined the Faculty of Oral Roberts University, Tulsa, Oklahoma, in August 1992, where he is currently an Assistant Professor of Engineering. His current research interests are in the dynamics, stability, and control of spinning rockets.

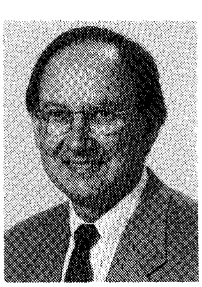

D. Lewis Mingori received his B.S. degree from the University of California, Berkeley, in 1960, his M.S. from the University of California, Los Angeles (UCLA), in 1962, and his Ph.D. from Stanford University (Aeronautics and Astronautics) in 1966. From 1966 to 1968 he was a member of the technical staff of the Aerospace Corporation, and since 1968 he has been a faculty member at UCLA. His teaching and research are in the areas of dynamics and control with applications primarily in the aerospace field. His research interests include spacecraft attitude control, spinning and dual-spin spacecraft dynamics, gravity-stabilized satellites, spinning rockets, control of flexible space structures, model reduction, and robust control.

Presented as Paper 92-4544 at the AIAA Guidance, Navigation, and Control Conference, Hilton Head, SC, Aug. 10–12, 1992; received Sept. 1, 1992; revision received Aug. 8, 1994; accepted for publication Jan. 15, 1995.

These issues may be investigated using a model consisting of a symmetric rigid body with axial thrust and an elastic, dissipative internal mass. The important parameters are the thrust level, spin speed, and inertia ratio of the rigid body and the characteristics and location of the spring–mass–damper. This analytical model is sufficient to provide insight into the first-order effects of mass motion, yet simple enough to allow stability results to be obtained in terms of the general design parameters of the system. This is accomplished using the second method of Lyapunov, in which the Lyapunov function is obtained by considering a general quadratic function of the states. Resulting analytical stability conditions are confirmed by simulation and agree with numerically obtained stability results for a similar system in which the mass motion was modeled by constrained planar pendula.[3]

Description of Model

The model used in this investigation is shown in Fig. 1. It is similar to the model analyzed in Ref. 1. but includes the effects of viscous damping forces due to the internal mass motion. The model consists of a symmetric rigid body (with mass center at point B) containing a mass particle (point P) that is constrained to move in a plane perpendicular to the symmetry axis of the body. Deviations of the particle position from the symmetry axis are denoted by the Cartesian coordinates x_1 and x_2, which are measured along the B_1 and B_2 axes, respectively. The transverse axes B_1, B_2 and the symmetry axis B_3 are fixed in the rigid body and pass through the point O, coinciding with the system mass center (point S) when x_1 and x_2 are zero. Movement of the particle away from the B_3 axis produces a linear elastic restoring force with spring constant k. When the particle is on the B_3 axis, it is a distance h away from the system mass center and the restoring force is zero. When the particle velocity relative to the rigid body is nonzero, a viscous damping force with coefficient c acts on the particle in a direction opposite to its velocity in the rigid body. A thrust vector F acts along B_3 and passes through the mass center of the rigid body. The thrust vector is a nonconservative force known as a follower force since it remains aligned with B_3 throughout the motion.

Similar models have been used to study the effect of liquified combustion products (slag) moving in a solid rocket motor casing onboard a spacecraft.[1,3] When the current investigation began, the particle was thought of as representing internal mass motion of a general type that could arise from several different sources. The intent was to investigate coning stability for a wide range of mass motion characteristics and rigid-body inertias. When it became apparent that mass motion under axial forcing could have a stabilizing effect on the coning motion of prolate spinning bodies, the investigation focused on the design and performance of a passive control device. In this application, the particle motion represents the mass motion of such a mechanism, hereafter called the passive coning attenuator (PCA).

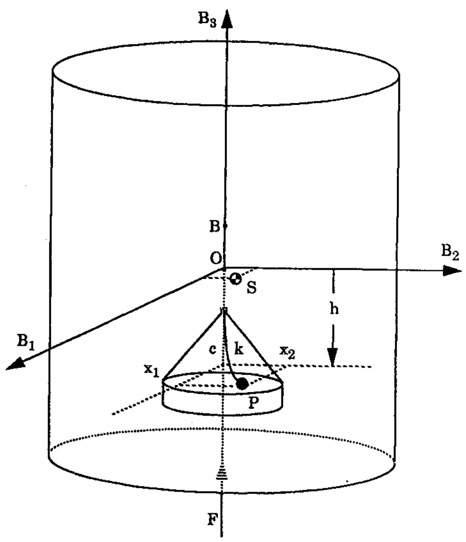

Fig. 1 Idealized spacecraft model.

An existing physical device that closely approximates the above model (for small-particle motions) is the elastic pendulum nutation damper. This device consists of a small mass fixed to one end of a relatively stiff wire. The other end of the wire is mounted inside a fluid-filled container that is in turn mounted in the spacecraft. Motion of the damper mass is excited by the nutational motion of the rigid body. The restoring force is furnished by the action of the wire being bent away from the symmetry axis. The damping force arises from the action of the viscous fluid on the mass as it moves relative to the container. For small deviations in mass position, the motion remains approximately in a plane perpendicular to the symmetry axis of the spacecraft. Although these devices were originally designed for use in spinning spacecraft without thrust, it will be shown that they can also be used to stabilize spinning, thrusting spacecraft if appropriately modified.

Linearized Equations of Motion

Four coupled linear differential equations are required to describe the transverse rotational motion of the spacecraft for small cone angles[1]:

$$\left(I_1 + mh^2\right)\dot{\omega}_1 + \left[I_3 - \left(I_1 + mh^2\right)\right]\Omega\omega_2 = 2\Omega mh\dot{x}_1 + mh\ddot{x}_2 - mh\Omega^2 x_2 - \mu F x_2 \tag{1}$$

$$\left(I_1 + mh^2\right)\dot{\omega}_2 - \left[I_3 - \left(I_1 + mh^2\right)\right]\Omega\omega_1 = 2\Omega mh\dot{x}_2 - mh\ddot{x}_1 + mh\Omega^2 x_1 + \mu F x_1 \tag{2}$$

$$\ddot{x}_1 - 2\Omega\dot{x}_2 - \Omega^2 x_1 + \frac{kx_1 + c\dot{x}_1}{m(1-\mu)} = \frac{-h}{1-\mu}(\dot{\omega}_2 + \Omega\omega_1) \tag{3}$$

$$\ddot{x}_2 - 2\Omega\dot{x}_1 - \Omega^2 x_2 + \frac{kx_2 + c\dot{x}_2}{m(1-\mu)} = \frac{h}{1-\mu}(\dot{\omega}_1 - \Omega\omega_2) \tag{4}$$

Variables not defined in the Nomenclature are defined in Fig. 1.

Before attempting to analyze the above equations, it is convenient to define some new parameters and variables. Let

$$\lambda = \frac{I_3 - I_1 + \mu mh^2/(1-\mu)}{I_1 - \mu mh^2/(1-\mu)}, \qquad \delta = \frac{mh^2}{(1-\mu)[I_1 - (\mu mh^2/(1-\mu))]} \tag{5}$$

$$\xi = \frac{c}{m(1-\mu)\Omega}, \qquad \gamma^2 = \frac{k}{m(1-\mu)\Omega^2} \tag{6}$$

$$z_i = \frac{(1-\mu)x_i}{|h|}, \qquad T = \frac{\mu F}{mh\Omega^2} = \frac{F}{(M+m)h\Omega^2} \tag{7}$$

$$r = \frac{h}{|h|} = \pm 1, \qquad \tau = \Omega t \tag{8}$$

Then, after some manipulation, the governing equations simplify to

$$\omega_1' + \lambda\omega_2 = r\delta\left[-\xi z_2' - (\gamma^2 + T)z_2\right] \tag{9}$$

$$\omega_2' - \lambda\omega_1 = r\delta\left[\xi z_1' + (\gamma^2 + T)z_1\right] \tag{10}$$

$$z_1'' - 2z_2' + \xi z_1' + (\gamma^2 - 1)z_1 = -r(\omega_2' + \omega_1) \tag{11}$$

$$z_2'' + 2z_1' + \xi z_2' + (\gamma^2 - 1)z_2 = r(\omega_1' - \omega_2) \tag{12}$$

where the prime denotes differentiation with respect to τ.

Solving Eqs. (9–12) for the highest derivatives and defining new parameters simplify the equations further to

$$\omega_1' = -\lambda\omega_2 - \Theta z_2 - \Phi z_2' \tag{13}$$

$$\omega_2' = \lambda\omega_1 + \Theta z_1 + \Phi z_1' \tag{14}$$

$$z_1'' = -\Lambda\omega_1 - \kappa z_1 - \Psi z_1' + 2z_2' \tag{15}$$

$$z_2'' = -\Lambda\omega_2 - \kappa z_2 - 2z_1' + \Psi z_2' \tag{16}$$

where

$$\Phi = r\delta\xi, \qquad \Theta = r\delta(\gamma^2 + T) \tag{17}$$

$$\Lambda = r(\lambda + 1), \qquad \kappa = \gamma^2(\delta + 1) + \delta T - 1 \tag{18}$$

$$\Psi = \xi(\delta + 1) \tag{19}$$

Let the state vector be defined as

$$x = [\omega_1 \quad z_1 \quad z_2' \quad \omega_2 \quad z_2 \quad z_1']^T \tag{20}$$

Then the governing equations can be written in matrix first-order form as

$$x' = Ax = \begin{bmatrix} 0 & 0 & -\Phi & -\lambda & -\Theta & 0 \\ 0 & 0 & 0 & 0 & 0 & 1 \\ 0 & 0 & -\Psi & -\Lambda & -\kappa & -2 \\ \lambda & \Theta & 0 & 0 & 0 & \Phi \\ 0 & 0 & 1 & 0 & 0 & 0 \\ -\Lambda & -\kappa & 2 & 0 & 0 & -\Psi \end{bmatrix} x \tag{21}$$

The equations are now in a convenient form for analysis.

Lyapunov Stability Analysis

It is desirable to have general analytical stability conditions under which the system represented by Eqs. (9–12) is asymptotically stable (i.e., all the eigenvalues of the A matrix lie in the left half of the complex plane). However, the system is sufficiently complicated to preclude solving for general expressions for the eigenvalues or even applying the Routh–Hurwitz criteria usefully. Therefore, the second method of Lyapunov was applied to the system. Consider the following stability theorems[4]:

Theorem 1. The null solution of the system $x' = f(x)$, $f(0) = 0$, is asymptotically stable if there exists a positive-definite function $V(x)$ such that $V'(x)$ is negative semidefinite, and there is no nonnull solution such that $V'(x)$ is identically zero.

Theorem 2. The null solution of the system $x' = f(x)$, $f(0) = 0$, is unstable if there exists a negative-definite or sign indefinite function $V(x)$ such that $V'(x)$ is negative semidefinite and there is no nonnull solution such that $V'(x)$ is identically zero.

These two theorems may be used to determine the necessary and sufficient conditions for asymptotic stability in terms of the general system parameters. The Lyapunov function is obtained via the following method.

Consider a Lyapunov function of the form

$$V(x) = x^T B x \tag{22}$$

where B is a constant, symmetric matrix containing 21 unknown elements. The time derivative of $V(x)$ for the differential equation (21) is

$$V'(x) = x^T C x \tag{23}$$

where

$$C = A^T B + BA \tag{24}$$

One way to find the elements of B is to postulate a form for C and then use Eq. (24) to determine the elements of B. Based on a desire to have V' reflect the dissipative nature of the system, the following form for $V'(x)$ was assumed:

$$V'(x) = -\Psi z_1'^2 - \Psi z_2'^2 \tag{25}$$

This V' represents the rate at which energy is removed from the system via damping. Since $\Psi > 0$ [see Eqs. (5), (6), and (19)], it follows that $V' \leq 0$. The C matrix corresponding to the V' given in Eq. (25) is

$$C = \begin{bmatrix} 0 & 0 & 0 & 0 & 0 & 0 \\ 0 & 0 & 0 & 0 & 0 & 0 \\ 0 & 0 & -\Psi & 0 & 0 & 0 \\ 0 & 0 & 0 & 0 & 0 & 0 \\ 0 & 0 & 0 & 0 & 0 & 0 \\ 0 & 0 & 0 & 0 & 0 & -\Psi \end{bmatrix} \tag{26}$$

In order to proceed with the stability analysis using Theorems 1 and 2, we must accomplish three tasks:

1) Determine whether $V' \equiv 0 \Rightarrow x = 0$.

2) Use Eq. (23) to find the matrix B corresponding to the A from Eq. (21) and the C from Eq. (26).

3) Test B for positive definiteness.

To accomplish step 1, substitute $z_1' = z_1'' = 0$ and $z_2' = z_2'' = 0$ into Eqs. (13–16) and see if there are any conditions under which nontrivial solutions exist. The result of this process is that no nontrivial solutions exist as long as

$$\lambda \neq \delta(\gamma^2 + T)/(\gamma^2 - 1) \tag{27}$$

We assume that this condition is satisfied in all subsequent analysis.

Accomplishing the second step involves constructing and solving 21 linear equations based on Eq. (24). Taking advantage of the sparseness of C and the inherent symmetry of the system and assuming that Eq. (27) is satisfied lead to the following form for B:

$$B = \begin{bmatrix} b_{11} & b_{12} & b_{13} & 0 & 0 & 0 \\ b_{12} & b_{22} & b_{23} & 0 & 0 & 0 \\ b_{13} & b_{23} & b_{33} & 0 & 0 & 0 \\ 0 & 0 & 0 & b_{11} & b_{12} & -b_{13} \\ 0 & 0 & 0 & b_{12} & b_{22} & -b_{23} \\ 0 & 0 & 0 & -b_{13} & -b_{23} & b_{33} \end{bmatrix} \tag{28}$$

The number of independent equations that must be solved then reduces to six:

$$\Phi b_{11} + \Psi b_{13} = 0 \tag{29}$$

$$\Phi b_{12} + \Psi b_{23} = 0 \tag{30}$$

$$\Theta b_{11} - \lambda b_{12} + \kappa b_{13} - \Lambda b_{23} = 0 \tag{31}$$

$$b_{12} - (\lambda + 2) b_{13} - \Lambda b_{33} = 0 \tag{32}$$

$$-\Theta b_{13} + b_{22} - 2b_{23} - \kappa b_{33} = 0 \tag{33}$$

$$\Phi b_{13} + \Psi b_{33} = \tfrac{1}{2}\Psi \tag{34}$$

Simultaneous solution of Eqs. (29–34) yields

$$b_{13} = -\frac{r(\delta + 1)(\lambda + 1)(\lambda - \delta)}{2\Delta} \tag{35}$$

$$b_{11} = -\frac{\delta + 1}{r\delta} b_{13} \tag{36}$$

$$b_{12} = -\frac{(\delta + 1)\sigma}{\lambda - \delta} b_{13} \tag{37}$$

$$b_{23} = \frac{r\delta\sigma}{\lambda - \delta} b_{13} \tag{38}$$

$$b_{33} = -\frac{(\lambda + 2)(\lambda - \delta) + (\delta + 1)\sigma}{r(\lambda + 1)(\lambda - \delta)} b_{13} \tag{39}$$

$$b_{22} = \frac{\delta\sigma[\lambda + 1 - T(\delta + 1)] - \Delta(\gamma^2 - 1)}{r(\lambda + 1)(\lambda - \delta)} b_{13} \tag{40}$$

where

$$\sigma = T + 1 \tag{41}$$

$$\Delta = (\lambda + 1)^2 + T(\delta + 1)^2 \tag{42}$$

Then from Eqs. (22) and (35–42), the Lyapunov function becomes

$$\begin{aligned} V = \frac{\delta + 1}{2\delta\Delta}\Big((\delta + 1)(\lambda + 1)(\lambda - \delta)\big(\omega_1^2 + \omega_2^2\big) \\ + \delta\{\Delta(\gamma^2 - 1) - \delta\sigma[\lambda + 1 - T(\delta + 1)]\}\big(z_1^2 + z_2^2\big) \\ + \delta[(\lambda + 2)(\lambda - \delta) + \sigma(\delta + 1)]\big(z_1'^2 + z_2'^2\big) \\ + 2r\delta\sigma(\delta + 1)(\lambda + 1)(\omega_1 z_1 + \omega_2 z_2) \\ - 2r\delta(\lambda + 1)(\lambda - \delta)(\omega_1 z_2' - \omega_2 z_1') \\ - 2\delta^2\sigma(\lambda + 1)(z_1 z_2' - z_2 z_1')\Big) \end{aligned} \tag{43}$$

With the B matrix known, the final step of the stability analysis is to determine the conditions under which B is positive definite. This can be done by examining the determinants of the principal minors of B. Three conditions are required for a positive-definite B:

$$b_{11} > 0 \tag{44}$$

$$\det\begin{bmatrix} b_{11} & b_{12} \\ b_{12} & b_{22} \end{bmatrix} > 0 \tag{45}$$

$$\det\begin{bmatrix} b_{11} & b_{12} & b_{13} \\ b_{12} & b_{22} & b_{23} \\ b_{13} & b_{23} & b_{33} \end{bmatrix} > 0 \tag{46}$$

Consider inequality (46) first. Multiply inequality (46) by the positive number Ψ and use Eqs. (29) and (30) to obtain (after some manipulation) another expression that is equivalent to inequality (46):

$$(\Phi b_{13} + \Psi b_{33})\big(b_{11}b_{22} - b_{12}^2\big) > 0 \tag{47}$$

In view of Eq. (34), inequality (47) reduces to

$$\Psi\big(b_{11}b_{22} - b_{12}^2\big) > 0 \tag{48}$$

Since Ψ is positive, Eq. (48) [and hence Eq. (46)] is satisfied if and only if Eq. (45) is satisfied. Thus, stability of the nominal motion is determined entirely by inequalities (44) and (45). Upon substitution from Eqs. (35–42), these inequalities become

$$\frac{\lambda - \delta}{(\lambda + 1)^2 + T(\delta + 1)^2} > 0 \tag{49}$$

$$[(\lambda + 1)^2 + T(\delta + 1)^2][\gamma^2(\lambda - \delta) - \lambda - \delta T] > 0 \tag{50}$$

Inequalities (49) and (50) together with the requirements that Ψ be positive and Eq. (27) be satisfied constitute the desired necessary and sufficient conditions for asymptotic stability. From these conditions, it is clear that there are four important parameters that need to be considered when establishing the stability characteristics of such a system:

1) The inertia ratio parameter λ of the system falls in the range $[-1, 1]$ for real systems [negative and positive values indicating prolate and oblate systems, respectively, see Eq. (5)]. For small m and h, λ is approximately $(I_3 - I_1)/I_1$.

2) The particle inertia δ about the body center of mass is normalized by the modified transverse inertia. This quantity would usually be small in practical applications.

3) The total vehicle acceleration T is the axial force magnitude divided by the total mass and is normalized by the spin speed squared times the axial offset of the particle.

4) The normalized spring stiffness γ^2 refers to the elastic restoring force on the particle.

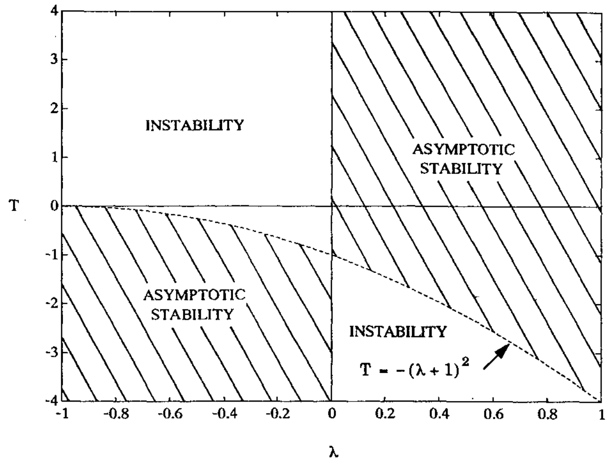

Fig. 2 Stability regions as δ approaches zero, $\gamma^2 > 1$.

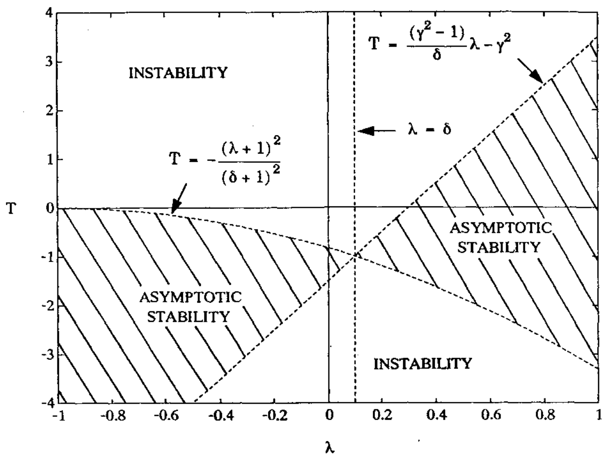

Fig. 3 Stability regions for $\delta = 0.1, \gamma^2 = 1.5$.

Consider the case of a prolate spacecraft (i.e., negative λ). Since δ is always positive, the numerator of inequality (49) is negative. Hence for stability, the denominator of inequality (49) must also be negative. This requires that T be negative (i.e., mass motion aft of the system mass center) and of sufficient magnitude (i.e., large enough thrust) to overcome the $(\lambda + 1)^2$ term. Furthermore, for inequality (50) to be satisfied, the spring stiffness must be large enough for $\gamma^2(\lambda - \delta)$ to overcome $-(\lambda + \delta T)$. Thus, qualitatively speaking, to stabilize the coning motion of a prolate spinner under thrust, viscously damped mass motion should be added aft of the system mass center, the thrust force must be sufficiently high, and the spring restraining the moving mass must be sufficiently stiff.

As δ approaches zero, conditions (49) and (50) reduce to

$$\frac{\lambda}{(\lambda + 1)^2 + T} > 0 \tag{51}$$

$$(\gamma^2 - 1)\lambda[(\lambda + 1)^2 + T] > 0 \tag{52}$$

For a constant $\gamma^2 > 1$, stability regions in the λ vs T parameter space are plotted in Fig. 2 based on conditions (51) and (52). Cross-hatched regions indicate asymptotic stability. All other regions are areas of instability. For comparison, stability regions in the same parameter space based on conditions (49) and (50) are shown in Fig. 3 for $\delta = 0.1$ and $\gamma^2 = 1.5$. As δ increases to a value of 0.2, the stability regions shrink to those shown in Fig. 4. If instead γ^2 is increased (to 2.0), the stability regions grow larger, as shown in Fig. 5. Refer to Fig. 3 to see the equations that describe the stability boundaries. These equations show how the boundaries will shift when the parameters change. The points on the straight-line stability boundary of Fig. 3 are exactly those points corresponding to condition (27). This combination of parameters must necessarily be avoided to achieve a stable design. It is interesting that in the case

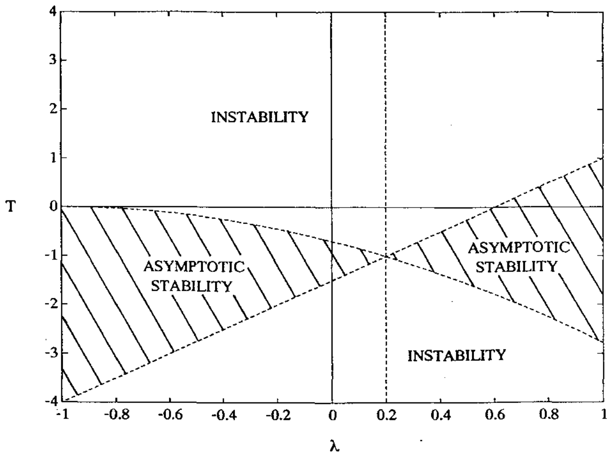

Fig. 4 Stability regions for $\delta = 0.2, \gamma^2 = 1.5$.

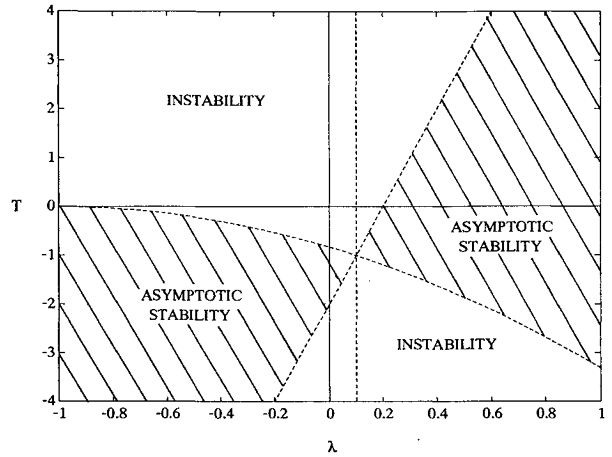

Fig. 5 Stability regions for $\delta = 0.1, \gamma^2 = 2.0$.

when δ approaches zero, stability is not possible anywhere in the parameter space if $\gamma^2 < 1$. In the case where δ is nonzero, there is also a critical value of spring stiffness that is required for stability. This value is characterized by the inequality

$$\gamma^2 > (1 - \delta)/(1 + \delta)^2 \tag{53}$$

which was obtained by reversing the trend exhibited in Fig. 5 (i.e., decreasing γ^2) until the stability regions vanish. This occurs when the straight-line stability boundary passes through the point $[\lambda = 1, T = -4/(\delta + 1)^2]$. Then the two stability boundaries intersect at $\lambda = \delta$ and also at $\lambda = 1$.

Design of Passive Coning Attenuator

In the preceding development, stability conditions have been obtained by assuming that the system is time invariant. In actuality, many of the parameters are not constant over the course of a solid motor burn. However, since the quantities change slowly relative to the period of a single spin cycle, it may be argued that the time-invariant analysis reasonably characterizes the stability at any particular point in time by considering the instantaneous parameter values at that time. The design of PCA to overcome a significant destabilizing effect must take into account all of the parameter values that may occur over the intended range of operation.

Of fundamental importance is the requirement that the stabilizing influence of the control device dominate the destabilizing influence throughout its intended range. Using a pendulum model of the slag phenomenon, the worst-case destabilizing time constant (occurring near the end of the burn) has been conservatively estimated at around 10 s for a 10-lb slag mass. The vehicle remains prolate but becomes less so during the burn. The inertia ratio parameter λ can vary as much as from -0.8 to -0.4. The thrust magnitude varies somewhat widely for different solid rocket motors and also varies somewhat over the course of the burn. In addition, the vehicle has a tendency to spin down during the burn. The magnitude of this variation is dependent on vehicle asymmetry and initial spin speed.

This dynamically changing system is to be stabilized by correctly locating and tuning a time-invariant mass–spring–damper system of the type analyzed previously. The tuning of the device refers to the design process by which its internal characteristics (mass, stiffness, and damping) are chosen so as to maximize its control effectiveness. To determine the spring stiffness, the natural frequency of the device is set equal to the nutation frequency of the vehicle at the worse-case condition where the destabilizing time constant is expected to be smallest. An approximate tuning is achieved by setting the natural frequency of the device equal to the nutation frequency of the unforced rigid body. This results in the following equation for γ^2:

$$\gamma^2 = \lambda^2 + 1 \tag{54}$$

An approximate expression for the damping time constant may be obtained from a perturbation analysis of the characteristic roots in which the parameter δ is assumed small but finite. Details of this analysis are presented in Ref. 5. If the stiffness parameter γ^2 is chosen in accordance with Eq. (54), the approximate damping time constant expression reduces to

$$\tau_D = \frac{(\xi^2 + 4)\lambda}{\delta\xi(\lambda + 1)[(\lambda + 1)^2 + T]} \tag{55}$$

By differentiating τ_D with respect to ξ and solving for ξ, one will find that a damping parameter of $\xi = 2$ minimizes the time constant. The two remaining design parameters to be chosen are the particle mass m and the distance aft from the system mass center to the point where the device is to be located (h). The damping time constant can be rewritten in terms of these parameters as

$$\tau_D = \frac{(1 - \mu)(\xi^2 + 4)I_T\Omega^2\lambda}{m\xi(\lambda + 1)\{[(\lambda + 1)\Omega h]^2 + Fh/(M + m)\}} \tag{56}$$

where

$$I_T = I_1 - (mh)^2/M \tag{57}$$

For physically reasonable values of the parameters m and $h (m < 0.05M, mh^2 < 0.2I_1)$, I_T and λ are relatively insensitive to changes in both m and h. Thus from Eq. (56) one can see that the value of m that minimizes τ_D is that which is as large as practically possible. The value of h that minimizes τ_D is

$$h = -\frac{F}{2(M + m)(\lambda + 1)^2\Omega^2} \tag{58}$$

In practice, this may yield a large magnitude for h, which may not be possible to achieve for a particular vehicle. In this case, h should be made as large as practically possible.

Numerical Examples and Simulation

The goal of the numerical analysis is to verify for specific parameter choices that a passive spring–mass–damper device can be designed to attenuate the coning of prolate spinners under thrust. This goal was accomplished by using a computer to calculate the eigenvalues and time response of a linear system consisting of a rigid body and two mass particles. Each particle was connected to the rigid body in the manner described in Fig. 1 and could be nominally located anywhere along the spin axis. This allowed for the parameters to be chosen so that one of the particles provides the dedamping effect whereas the other particle represents the passive damping device. Initially, the parameters for modeling the dedamper were taken from the slag model of Mingori and Yam.[1] The model is the same as that described in this paper except that there is no viscous damping on the particle. The inertias and mass center location were also taken from the model of Ref. 1, which was based on typical flight data.

Parameter values were taken from a point in the example trajectory of Ref. 1 near the end of the burn ($t = 60$ s). The dedamping time constant for nutation (the inverse of the real part of the eigenvalue corresponding to nutational motion) at the point was found to

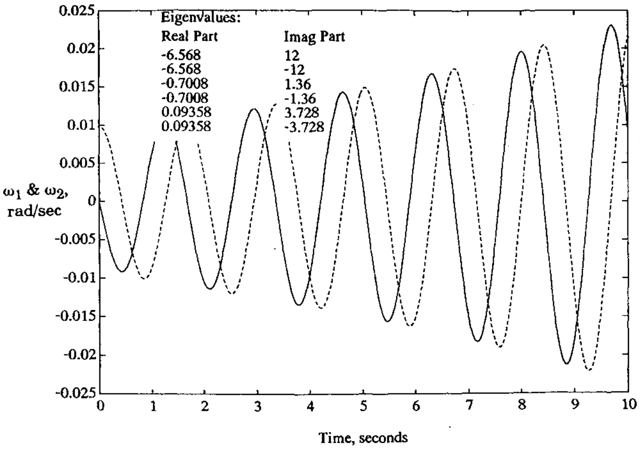

Fig. 6 Time response with dedamping particle only.

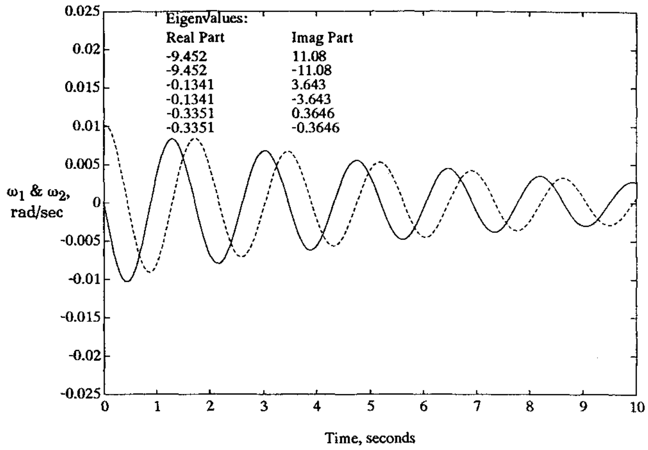

Fig. 7 Time response with damping particle only.

be about 10 s. Dedamping time constant values at points later in the burn were found to be overly pessimistic (2.5 s at $t = 70$ and 1.6 s at $t = 85$). Using the design procedure presented in the previous section, parameter values for a passive control device were found to damp nutational motion in the presence of this dedamper. However, a very large particle mass value (nearly $0.2M$) was necessary. Furthermore, although the nutation root was brought into the left-half plane by the addition of the damping device, no amount of passive damping was found to stabilize (move into the left-half plane) the root corresponding to the undamped oscillator. It is believed that this dedamper is inherently unstable due to the specific choice of parameters.[1] This is consistent with the choice of $\gamma^2 = 0.25$, which results in a soft spring. It was found that if γ^2 was increased slightly with all other parameters held constant, the oscillator became stable and lost its dedamping effect on the body. Relationships between Ref. 1 and the current work are discussed in Ref. 6.

To further investigate the damping characteristics of the PCA, a second type of dedamper was modeled. This dedamper was characterized by a viscously damped mass particle connected to the rigid body by a stiff spring. This is the same type of oscillator that has been used thus far to model the passive damper. In locating it forward of the system mass center, it provides a destabilizing influence on the body as predicted in the analysis section. A choice of parameters was found that provided a dedamping nutation time constant of about 10 s. With this type of dedamper, a considerably smaller particle mass value ($<0.05M$) was needed to stabilize all the eigenvalues. Numerical studies showed that a damping device resulting in a nutation time constant of 8 s (without the presence of a dedamper) provided an overall damping time constant of 50 s when combined with a 10-s dedamper of this type. The eigenvalues and transverse rates for each case are shown in Figs. 6–8. The angular velocity measure numbers for the B_1 and B_2 axes are given by solid and dashed lines, respectively. In Fig. 6, the dedamper characteristics are $m = 73$ kg (5 sl), $h = 1.5$ m (5 ft), and $\gamma^2 = 1.25$. In Fig. 7, the damper characteristics are $m = 58$ kg (4 sl), $h = -2.4$ m (-8 ft), and $\gamma^2 = 1.10$. Both the damper and dedamper have a damping coefficient of $c = 438$ kg/s (30 sl/s) and their combined effect is shown in Fig. 8.

The PCA was found to provide considerable damping effects for much smaller particle mass values as well. Through numerical studies it was found that performance is improved if the damper is split up into four smaller, off-axis devices in which each mass is constrained to one-dimensional motion. The configuration is similar to that shown in Fig. 9 except that all four masses may oscillate. With this configuration a damping time constant of 5.5 s was achieved with a total mobile mass value as small as $0.005\,M$, assuming the devices could be placed 7.3 ft aft of the system mass center. This time constant value was achieved in the absence of a dedamper.

The validity of the previously described linear model has been confirmed by computer simulation of the full nonlinear equations for the case of the rigid body with two particles attached. It was found that the transverse rates of the linear and nonlinear models did not exhibit significant disagreement until nutation angles of over 10 deg

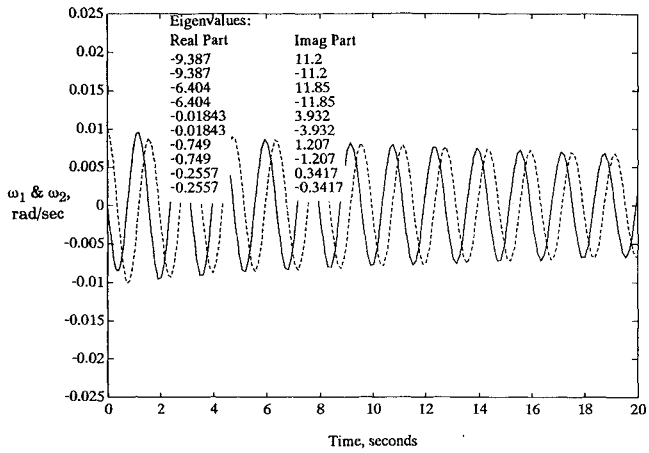

Fig. 8 Both damping and dedamping particles from Figs. 6 and 7.

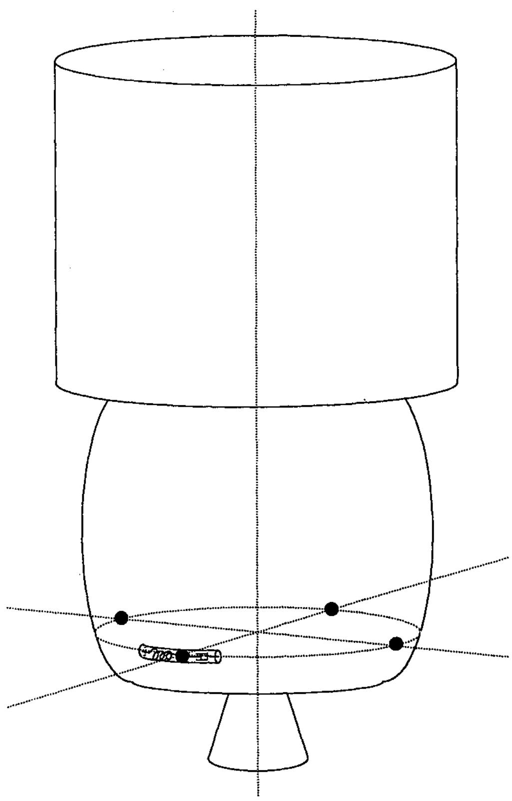

Fig. 9 Balanced off-axis PCA with one-dimensional constrained particle motion.

were simulated.[5] These results confirm that the linear model is an accurate representation of the actual system for small cone angles.

Discussion

Although the mass–spring–damper model presented here may not be an accurate representation of the slag sloshing phenomenon, it is certainly a reasonable model of a passive control device similar to a type currently in use for spinning spacecraft without thrust. The only approximations that have been made are the linearization of the governing equations and the time invariance assumption on the parameters. These approximations are necessary to retain simplicity and hence gain insight into the behavior of the system. It is believed that the actual time-varying parameters change so slowly that the stability characteristics derived from a time-invariant analysis persist in reality.

Although an extremely large damper was necessary for overcoming the coning instability induced by the soft spring–mass dedamper, this does not belie the potential of the PCA as a solution to the slag coning instability problem. As was shown by numerical studies, a much smaller damper was required to stabilize a different type of dedamping mechanism with the same dedamping time constant as that of the soft spring system. Since the dedamping mechanism for the coning instability is as yet unknown, it is possible that the PCA could provide a feasible alternative to the active nutation control systems currently used. Since the PCA must be located some distance aft of the system mass center, it may need to be placed off the center line of the vehicle. This is because it is impractical to locate such a device within the solid rocket motor casing. This is not expected to be a problem since the moving mass can be balanced symmetrically by motionless (or moving) particles of equal mass located elsewhere on the vehicle. This concept is illustrated in Fig. 9. An analytical model of the off-axis damper has been studied, and it has been verified that the desirable damping properties are retained with essentially the same stability characteristics.[5]

In other examples, relatively small values of mass were shown to be capable of providing significant damping characteristics. Thus the PCA has potential to be used in cases where the dedamping effect is not as pronounced as in the slag coning instability. Perhaps coning due to structure flexibility or liquid propellant sloshing during a longer thrust period could be stabilized by only a relatively small damping device. The value of this type of simple, passive stabilization concept is that it can be applied to any thrusting, spinning, symmetric body to enhance coning stability.

One of the difficulties that arises with the application of a PCA is that, although stable in the high-thrust regime, the same mass motion contributes to greater instability in the low- (or no-) thrust regime. This is an inherent characteristic that is evident from the stability results derived herein and cannot be avoided. With regard to the slag coning instability, this difficulty may be circumvented by strapping the device to the outside of the motor case. Thus, the device will be ejected with the spent motor after the burn. However, this solution does not address the coast periods prior to the burn or after the burn and prior to motor separation. Of course, the problem is resolved if one is able to cage and uncage the mass upon command from the ground. However, this is a capability that may be too complicated or costly to provide in practice. A more ingenious way of overcoming this difficulty is to take advantage of the high acceleration level being induced during thrust to automatically uncage the oscillator. Likewise, at the end of the thrust period, the acceleration would cease and the oscillator would automatically be caged. This is accomplished by connecting the mass to the rigid body with an additional spring (aligned with the thrust axis) that nominally holds the mass at the narrow end of a funnel-shaped compartment but extends under thrust to allow the mass to wander about the open end of the compartment. This quiescently caged oscillator concept (illustrated in Fig. 10) solves the low-thrust instability problem passively.

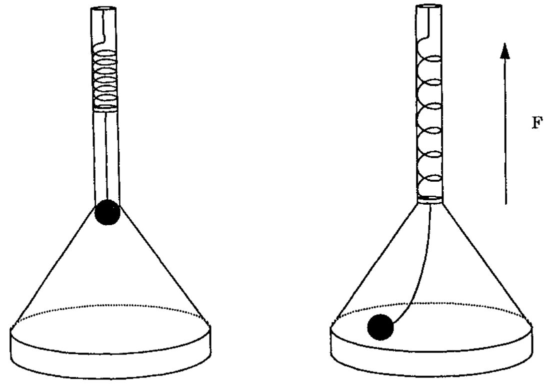

a) Low or no thrust b) High thrust

Fig. 10 "Quiescently caged" oscillator.

Conclusions

Necessary and sufficient analytical conditions for asymptotic stability have been derived for symmetric spinning bodies with axial forcing and dissipative internal mass motion. These conditions show that spin about the minor axis can be made asymptotically stable if the thrust is large enough, the spring is stiff enough, and the mass motion occurs aft of the system mass center. The simplicity of the resulting conditions provides insight into how to design and locate a passive control device to stabilize prolate spinners under thrust. Numerical studies have confirmed the analysis to show that for specific parameter choices strong dedamping influences can be overcome by implementing a passive control device designed by such methods.

References

[1]Mingori, D. L., and Yam, Y., "Nutational Instability of a Spinning Spacecraft with Internal Mass Motion and Axial Thrust," *AIAA Astrodynamics Conference Proceedings* (Williamsburg, VA), AIAA, Washington, DC, 1986, pp. 367–375 (AIAA Paper 86-2271).

[2]Ancher, L. J., Brink, H., and Pouw, A., "Study on Passive Nutation Dampers," (in 3 volumes), ESA Contractor Report CR(P)-788, Noordwijk, Holland, Dec. 1975.

[3]Or, A. C., "Rotor-Pendulum Model for the Perigee Assist Module Nutation Anomaly," *Journal of Guidance, Control, and Dynamics*, Vol. 15, No. 2, 1992, pp. 297–303.

[4]Hughes, P. C., *Spacecraft Attitude Dynamics*, Wiley, New York, 1986.

[5]Halsmer, D. M., "Nutational Stability and Passive Control of Symmetric Spinning Bodies with Axial Forcing and Internal Mass Motion," Ph.D. Dissertation, Univ. of California at Los Angeles, CA, 1992.

[6]Mingori, D. L., Halsmer, D. M., and Yam, Y., "Stability of Spinning Rockets with Internal Mass Motion," presented at AAS/AIAA Spaceflight Mechanics Meeting, Pasadena, CA, Feb. 22–24, 1993.